Experimental characterization of the dynamic thermal properties of opaque elements under dynamic periodic solicitation

Giovanni Pernigotto – University of Padova, Vicenza, Italy – pernigotto@gest.unipd.it
Alessandro Prada – Free University of Bozen-Bolzano, Bolzano, Italy – alessandro.prada@unibz.it
Francesco Patuzzi – Free University of Bozen-Bolzano, Bolzano, Italy – francesco.patuzzi@unibz.it
Marco Baratieri – Free University of Bozen-Bolzano, Bolzano, Italy – marco.baratieri@unibz.it
Andrea Gasparella – Free University of Bozen-Bolzano, Bolzano, Italy – andrea.gasparella@unibz.it

Abstract

A modified hotbox facility has been used at the Free University of Bozen-Bolzano to measure heat fluxes under a periodic pulse solicitation for some timber structures with different number and kind of layers. The simplest one – a single layer timber structure, has also been modelled with ANSYS Fluent® and the results compared to the experimental data for validation. Then, the numerical model has been used to study different forcing signals and boundary conditions. In order to characterize the response to a periodic dynamic solicitation with simple indexes, the EN ISO 13786:2007 (CEN, 2007) dynamic parameters have also been calculated.

1. Introduction

The increasing use of building energy simulations, *BES*, is bringing new solutions, aimed at exploiting the dynamic behaviour of the building envelope in order to improve its energy efficiency and the occupants' comfort. However, some hypotheses adopted in *BES* for the modelling of the elements of the opaque components (e.g., homogeneous layer with constant and isotropic thermal conductivity) can be very inaccurate for some kind of walls, such as those with air gaps or innovative materials. In this perspective, experimental methods can be the most effective approach to characterize dynamic thermal behaviour and to quantify it by means of simple parameters, such as periodic thermal transmittance, decrement factor and time shift defined by EN ISO 13786:2007.

While technical standards, such as EN 1934:1998 (CEN, 1998) and the literature (Asdrubali and Baldinelli, 2011) can provide instructions and examples about the measurement of the steady state heat transfer properties, there are no established references for the evaluation of wall dynamic behaviour by means of experimental laboratory tests.

In order to measure time shift and decrement factor, Ulgen (2002) built a simulation unit consisting of two volumes separated by the wall specimen: in the first one, adiabatic boundaries and no heat generation were realized while in the other one a sinusoidal temperature signal was generated. Sala *et al.* (2008) modified a calibrated guarded hotbox unit to measure the dynamic thermal properties of insulated brick walls. They used a triangular solicitation of 10°C amplitude and a 2 h period as forcing temperature. Moreover, they compared the results also with finite volume simulation. From the experimental output of the same apparatus, Martìn *et al.* (2010) calculated also wall response factors without any measurement of the material properties. By means of an adiabatic hotbox apparatus, Yesilata and Turgut (2007) compared effective thermal transmittances of both isotropic (e.g., ordinary concrete) and anisotropic building materials (e.g., rubberized concrete). More recently, Sun *et al.* (2013) and Ferrari and Zanotto (2013) measured the time shift and the decrement factor in laboratory by artificially reconstructing the profiles of external air temperature.

Despite the number of examples, no standard procedure is given. Moreover, a detailed evaluation of error propagation in modified hotbox apparatus is

still missing, especially regarding the boundary conditions to which the wall specimen is exposed during a dynamic test. If the aim of the test rig is to measure EN ISO 13786:2007 dynamic parameters, then the standard also provides the boundary conditions to apply – constant temperature on one side and sinusoidal forcing temperature on the other one. However, it could be challenging to keep the air temperature constant and to realize a sinusoidal forcing signal in practice. As explained by Prada *et al.* (2013), the encountered difficulties in designing a modified hotbox for dynamic tests brought to choose a different kind of forcing signal and to use numerical techniques to extract the first harmonic (i.e., the part of the output signal originated by a sinusoidal input signal) from the whole measured heat flux. In this research, with the support of finite volume simulation models calibrated with experimental results, we discussed the effectiveness of the implemented experimental procedure and we analysed the main sources of errors due the imposed boundary conditions.

2. Experimental and numerical methods

2.1 Hotbox apparatus description

The hotbox apparatus at the Free University of Bozen-Bolzano was designed according to EN 1934:1998 to perform steady state tests and consists of two insulated boxes (170 cm of height/width and 110 cm of length) made by aluminium plates filled with 10 cm of polyurethane insulation. The square specimen (with a side of 150 cm) is positioned to complete the open side of the two boxes.

In each box, a black screen (thickness 1.5 cm) separates the inner zone from the air gap zone of 3.9 cm adjacent to the test wall. In this way, heat exchange by radiation between the hotbox internal surfaces and the specimen is prevented. Moreover, a cylindrical horizontal fan generates a regular-shaped airflow stream in the air gap, flowing from the bottom to the top of the sample surface and reducing issues of vertical air temperature stratification. Each box is equipped with a cooling unit (an evaporator) and a heating unit (an electrical resistance), which are controlled by a PID regulation unit, tuned up to keep an internal constant temperature in a range of ± 0.1°C with respect to the setpoint temperature in steady state test. For the measurement of the wall thermal conductance in steady state tests, both chambers are kept at constant temperatures (generally 20°C and -10°C, respectively). The thermal flux is measured on a central square section (50 cm by 50 cm).

For dynamic tests, the configuration is modified and only one chamber is used, to maintain steady state conditions on one side of the specimen (i.e., the internal side). In order to impose the forcing temperature signal on the other side (i.e., the external side), a copper coil electrical heater of around 120 x 120 cm is positioned very close to the wall surface. This allows us to minimize air buoyancy effects, which could cause temperature gradients between the bottom and the top parts. The electrical heater can generate a nominal thermal power of 1500 W.

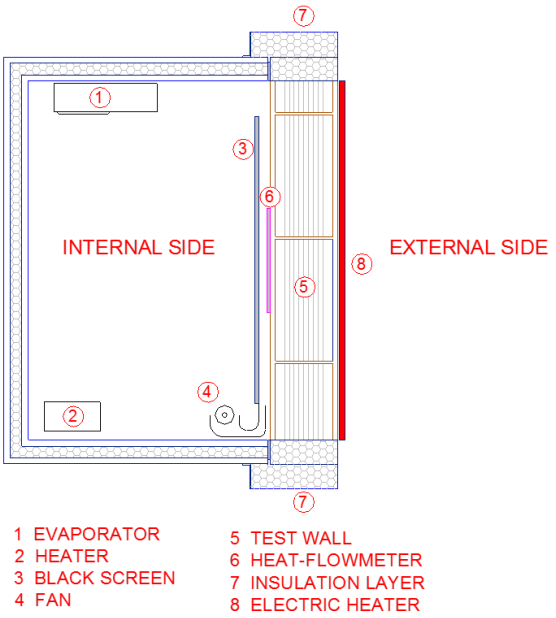

Fig. 1 – Modified hotbox apparatus.

As in the steady state tests, the heat flow variations on the internal side of the component are measured with a heat flow meter, *HFM*, namely a thermopile made of 250 type T thermocouples on an area of 50 x 50 cm. It consists of a layer of rubber of 1.05 cm between two layers of aluminum (thickness 0.1 cm), for a total mass of 2.3 kg. According to the calibration certificate, *HFM* thermal conductivity is

0.1905 W m^{-1} K^{-1}. A guard ring with similar thermal resistance surrounds the *HFM*. 8 and 4 type T thermocouples measure, respectively, the temperature of the wall surface in touch with the guard ring and that in touch with the *HFM*. On the external side, 12 thermocouples are placed in the same positions, 1 mm under the external surface of the specimen, in order to avoid the influence of direct irradiation due to the electrical heater.

2.2 Experimental procedure for the evaluation of dynamic parameters

During the dynamic tests, the internal side temperature is held at a constant value: specifically, for this work, a setpoint of 23°C was considered in order to minimize the heat exchanges with the environment. The airflow rate was set to 1.5 m s^{-1} and the relative humidity was not controlled. A dynamic test starts once steady state conditions are realized and this requires, typically, 24 h. Then, the external side is exposed to cycles of thermal irradiation of 1500 W for 2 h followed by 22 h of rest. A test can require repeating the cycles of forcing irradiation for two weeks (e.g., 14 times), depending on the kind of examined walls. This is necessary both for the minimization of the influence of the initial conditions and for the achievement of steady periodic conditions. For the specimen analysed in the present research, 10 days were sufficient. In particular, the transient effects were negligible after a couple of days but usually 3 or 4 days are required. Once the steady periodic state is reached – i.e., when the amplitude of the thermal flux is constant between two periods – the heat flux on the internal side and the external surface temperatures is recorded.

The Fast Fourier Transform (*FFT*) algorithm (Press *et al.*, 2007) is applied, computing the first 720 harmonics of experimental temperature and heat flux per each day of recorded series. The first term of the Fourier approximation is then used to compute the periodic thermal transmittance and the time shift according to EN ISO 13786:2007. Actually, since surface heat fluxes and temperatures are directly measured and used in calculations, the surface resistances are neglected and, thus, the estimated quantity is a periodic thermal transmittance without the effects of surface resistances.

The periodic thermal transmittance Y_{ie} is computed as the ratio between the amplitude of the first harmonic of the internal heat flux $\phi_{i,1}$ and the amplitude of the first harmonic of the external surface temperature $\theta_{e,1}$.

$$Y_{ie} = \frac{\phi_{i,1}}{\theta_{e,1}} \quad (1)$$

The time shift Δt_{ie} is calculated using the phase displacements (respectively, φ and ψ) of the first harmonics.

$$\theta_e \approx \bar{\theta}_e + \theta_{e,1} cos(\omega t + \varphi) \quad (2)$$

$$\phi_i \approx \bar{\phi}_i + \phi_{i,1} cos(\omega t + \psi) \quad (3)$$

$$\Delta t_{ie} = \frac{\psi - \varphi}{\omega} = \frac{\psi - \varphi}{2\pi} \times 24\ [h] \quad (4)$$

Y_{ie} and Δt_{ie} are determined for each day of the series of recorded data after the periodic steady state condition is reached. From the sample of daily dynamic parameters, mean values and standard deviations are calculated and presented.

2.3 Experimental specimens

Some timber walls have been tested according to the described procedure. For example, in a previous work (Prada *et al.*, 2013) the dynamic performance of two platform frame timber walls were presented. The two specimens were first tested according to EN 1934:1998 in order to determine their thermal conductance C_s and then according to the proposed procedure to estimate periodic thermal transmittance and time shift (specimens 1 and 2 in Tab. 1). However, the considered walls were too complex to analyze the inaccuracy introduced by the boundary conditions, because of the uncertainty of the material properties of many different layers. For this reason, we selected a new specimen (3 in Tab. 1): a single-layer wall of massive timber with a thickness of 24 cm. Also in this case the thermal properties were unknown. Nonetheless, being the specimen composed by a single material, it was possible to perform more efficiently a numerical model calibration from experimental measures.

Table 1 – Experimental analysis of the previous (1 and 2) and current (3) specimens.

Wall	C_s [W m^{-2} K^{-1}]	Y_{ie} [W m^{-2} K^{-1}]	Δt_{ie} [h]
1	0.172	0.031	9.18
2	0.240	0.101	6.73
3	0.475	0.130	11.64

As it can be seen, both thermal conductance and periodic thermal transmittance of specimen 3 are larger than those of 1 and 2. It means that this wall can be more susceptible to the choice of the forcing signal and to the generated external surface periodic temperature, making it more suitable for the purpose of our analysis.

2.4 Numerical simulation models

2.4.1 Definition and calibration of the numerical model

A numerical model has been defined and calibrated, considering both a proper abstraction level and the characterization of the unknown material properties. The outcome of this first part was a numerical model able to simulate the specimen behavior in the modified hotbox apparatus and under the test conditions. Since the final aim of the dynamic test rig is to measure EN ISO 13786:2007 dynamic parameters, the values shown in Tab. 1 were considered as calibration targets, with an acceptable tolerance of approx. 5 %. Moreover, since the measurement approach relies on *FFT* calculations on the monitored heat flux, the first harmonic signals from numerical results were calculated as well and compared to the experimental ones.

As regards the numerical aspects, ANSYS Fluent® finite volume approach with conjugated heat transfer modelling between solid and fluid regions was chosen. For the flow model, since the fan operates at constant velocity and there is low turbulence in the air gap adjacent to the specimen, Fluent DNS was used. The radiative heat exchange was calculated by means of the surface-to-surface model. Some preliminary tests were performed in order to balance numerical errors and computational costs, optimizing meshing, time-discretization and convergence criteria. In the final model, the mesh has more than 21000 quadrilateral cells and the transient problem is solved considering a time-discretization of 60 s, which is the same time between two consecutive measurements in the experiments. A convergence criterion of $\mathcal{E} = 10^{-8}$ was adopted and the simulations were run with double precision solver.

2.4.2 Geometric modelling and boundary conditions

As far as the simplification level is concerned, we adopted a 2D approach: indeed, the hotbox facility is well insulated and the heat flows through the lateral walls of the specimen, including its surrounding 20 cm of EPS and the additional 10 cm of sheep wool, are negligible. Similarly, the same is true for the heat flows through the bottom and the top wall surfaces and this allowed us to impose adiabatic boundary conditions.

In order to delimit the thermo-dynamic system, we focused on the specimen and on its adjacent zones. We defined the external wall surface exposed to the electrical heater as a solid domain boundary and used the measured surface average temperature as boundary condition. Considering the vertical length of the domain, we chose to have the same length of the heater (i.e., 120 cm). On the top and the bottom of the heater, as well as on the lateral sides, the surface temperature is slightly different from the average value because of border effects. Nonetheless, since our aim is to compare the heat flux where the *HFM* is installed (i.e., centered with respect to the electrical heater), the introduced inaccuracy is expected to be negligible. On the internal side, the air gap between the black screen and the specimen was included in the numerical model as a fluid domain and the measured temperature of the incoming air used as input. The inlet boundary was modelled as a velocity inlet while the outlet boundary as an outflow condition. The border effects were not included in the model but they are supposed to have low impact on the measurement area, whose lower and upper sides are 36 cm far from air inlet and outlet, respectively. The black screen was included as solid domain in order to account for the radiative exchanges on the internal side of the specimen. A boundary conditions of 23.7°C (i.e., the average measured temperature of the chamber internal air for the current experimental

campaign) was imposed on the side faced towards the rest of the chamber and adiabatic conditions were set on top and bottom surfaces.

In the experimental setup, the internal side of the specimen is not directly exposed to the air gap because of the *HFM* and its guard ring. We performed some preliminary tests without modelling *HFM* and guard ring but the numerical heat flow resulted influenced by the instability of air gap temperature more than it was actually in the experimental data. This suggested that *HFM* disturbs the measurement in such a way to require its modelling, together with the guard ring. Perfect contact (i.e., no contact resistance) was assumed between guard ring and *HFM* and between the two of them and the internal side of the specimen. Adiabaticity was imposed to top and bottom surfaces of the guard ring, coherently with the assumptions for both specimen and black screen.

2.4.3 Material properties

Some material properties were unknown but only those that have a significant impact on the dynamic parameters of the specimen were considered for calibration.

The black screen is in plywood and the same first-run properties of the specimen were assumed, together with a unitary surface emissivity. However, since the difference between the boundary temperature and the average air gap temperature is around 0.4°C and the black screen temperature is very stable during the simulation, no further in-depth analysis was performed. Indeed, the introduced error affects the mean value of the heat flux and not its shape and, thus, not the dynamic parameters, which are the actual calibration target.

For the *HFM*, the data from its calibration certificate were used to estimate the material properties: thermal conductivities of 202 W m^{-1} K^{-1} and 0.16 W m^{-1} K^{-1}, specific heat capacities of 871 J kg^{-1} K^{-1} and 840 J kg^{-1} K^{-1} and densities of 2719 kg m^{-3} and 360 kg m^{-3} were used, respectively, for aluminum and rubber layers. For the guard ring, the same thermal conductivity of the *HFM* was used. Density and specific heat capacity were unknown and values of 1000 kg m^{-3} and 840 J kg^{-1} K^{-1} were considered for the first-runs. We observed that the penetration depths of the harmonics of the forcing solicitation were clearly influenced but this affected marginally the measurement area. Consequently, we decided to concentrate our calibration efforts on the specimen and to consider a more accurate characterization of the guard ring in the future developments. For all surfaces exposed to the air gap an emissivity of 0.9 was assumed.

As far as the specimen is concerned, we used constant properties, as done for the other solid domains. This assumption can introduce some discrepancies because the temperature in some regions of the domain ranges from 20°C to 50°C. From the experimental thermal conductance (Tab. 1), a thermal conductivity of 0.114 W m^{-1} K^{-1} was determined. Further developments are likely to include thermo-physical properties function of the temperature, using the measurements from other experimental devices (e.g., laser flash, LFA, tests for thermal diffusivity). Once defined the thermal conductivity, the specific heat capacity and the density were varied in ranges admissible for timber structures, i.e., respectively, from 1000 to 2000 J kg^{-1} K^{-1} and from 300 to 400 kg m^{-3}, starting from the lower values. Specimen material properties compatible with our targets were found to be a thermal conductivity of 0.114 W m^{-1} K^{-1}, a specific heat capacity of 2000 J kg^{-1} K^{-1} and a density of 300 kg m^{-3}.

2.4.4 Simulated cases

First, we focused on the actual shape and on the errors in the repetition of the forcing signal (i.e., in realizing each day the same forcing condition). For this reason, we performed two simulations: in case (a) the series of daily first harmonic of the external surface temperature as forcing signal are considered; in case (b) a single average sinusoidal temperature perfectly repeated for ten days is imposed. In order to investigate the effect of actual instable internal air temperature, the same cases were run again considering constant internal conditions: specifically, case (c) has the same external surface temperature of case (a) and case (d) the same single average sinusoidal of case (b).

The second part of our analysis was dedicated to the numerical assessment of the role of the shape of the forcing signal, validating the findings of the first part. Two new forcing surface temperatures were

considered: a square (1) and a triangle wave (2) built from the same average sinusoidal applied in cases (b) and (d) (Fig. 2). As a whole, considering both actual and constant internal air temperature conditions - respectively, groups (b) and (d), four new cases were simulated and discussed.

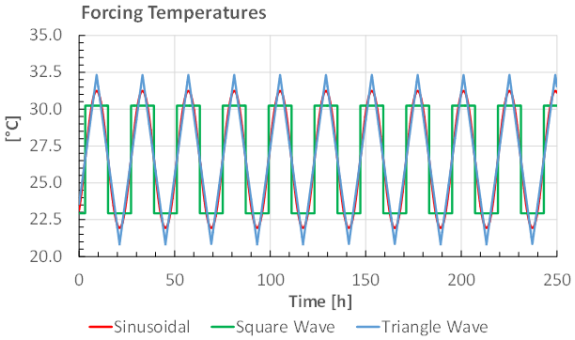

Fig. 2 – Sinusoidal, square and triangle external surface forcing temperatures.

3. Results and discussion

3.1 Calibrated numerical model

Measured and numerical heat fluxes have different average values ($\Delta\phi \approx 1$ W m^{-2}) but similar shapes (i.e., very close amplitudes and small differences between phases). For example, this can be seen for the days IV and V of the data series in Fig. 3, where the measured heat flux, both the original signal and the one processed with a second order Butterworth low-pass filter, is represented on the left vertical axis and the numerical heat flux on a right vertical axis that is shifted of 1 W m^{-2} with respect to the left one.

The first harmonics from *FFT* analysis confirm the findings from the comparison of the whole heat fluxes: regarding the amplitude, the average deviation from the 3rd to the 10th day (i.e., in periodic steady conditions) is 0.01 W m^{-2} (i.e., 2 %) while for the phase the average deviation is 0.19 rad (i.e., 2.8 %). The numerical average Y_{ie} and Δt_{ie}, are 0.133 ± 0.10 W m^{-2} K^{-1} and 10.97 ± 0.54 h – very close to the experimental ones (respectively, 0.130 ± 0.07 W m^{-2} K^{-1} and 11.64 ± 0.29 h).

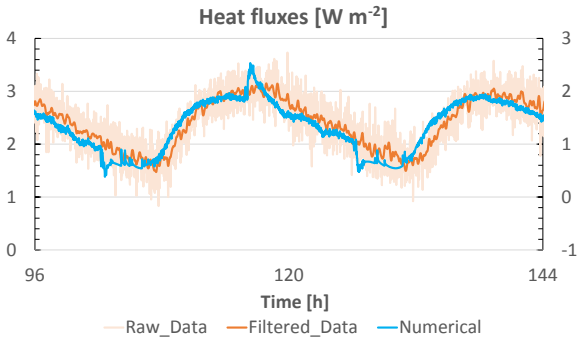

Fig. 3 – Overlapped experimental and numerical heat fluxes for day IV and V. Experimental raw and filtered data are represented on the left axis and the numerical data on the shifted right axis.

With the considered material properties, the analytical values of Y_{ie} and Δt_{ie} are 0.153 W m^{-2} K^{-1} and 9.89 h. This means that experimental and numerical periodic thermal transmittance are -15% and -13% lower and time shifts are +18% and +11% higher than the corresponding analytical values. Since both experimental and numerical approaches lead to similar results, some other elements and errors besides material uncertainty influence the accuracy of the experimental procedure adopted for the evaluation of EN ISO 13786:2007 wall dynamic parameters.

3.2 Analysis of the boundary conditions

According to the theoretical conditions prescribed by EN ISO 13786:2007, we should keep a constant temperature on the internal side and a sinusoidal forcing signal on the external side of the specimen.

Regarding the internal side, we observed that when the experimental apparatus is modified to perform dynamic tests, its control system is still not optimized to keep a constant internal temperature. For the current test, the average air gap temperature is 23.3 ± 0.1°C but, as shown in the graph on the top of Fig. 4, there are peaks and minimums as an effect of the hotbox heating and cooling units turning on and off.

On the other hand, the operating cycles of the electrical heater realize an external surface temperature far from being sinusoidal. Moreover, no pair of consecutive days has exactly the same forcing signal because of the variations of the lab air temperature. This means that boundary conditions do not perfectly comply with those of a periodic steady state regime. However, as it can be seen in the bottom graph of Fig. 4, the series of the daily first harmonics of the external surface temperature are very close to the sinusoidal function developed from

their average phase and amplitude. Analysing the daily first harmonics of the heat flux from day III to X, we can see differences from one day to another both in experimental and calibrated models (Fig. 5).

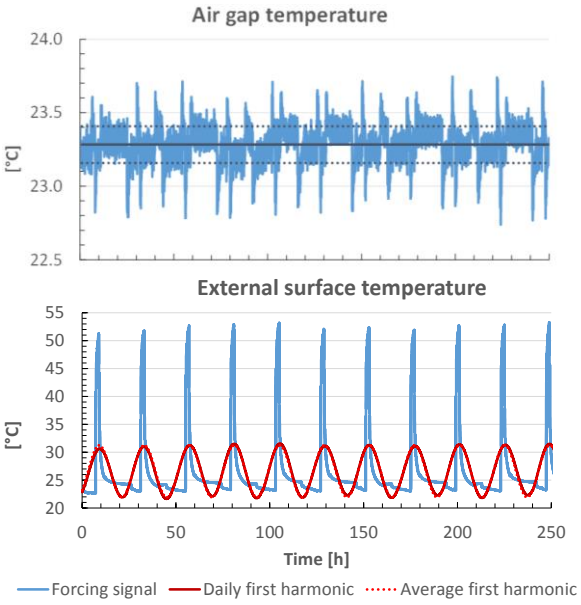

Fig. 4 – Air gap temperature and external surface temperatures from day I to X.

In numerical case (a), applying the series of first harmonics instead of the external surface temperature, the differences between the days decrease but, even using the same sinusoidal signal repeated 10 times in case (b), they do not disappear (Fig. 5). In case (c), differently from case (a), a constant internal air temperature is set and some improvements can be found. Finally, in case (d), which respects the conditions prescribed by the theoretical method, each period has exactly the same first harmonic signal of the monitored heat flux. That suggests that not only the shape and the errors in the replication of the external surface temperature affect the monitored heat flux and the outcome of *FFT* analysis but also the non-constant internal conditions.

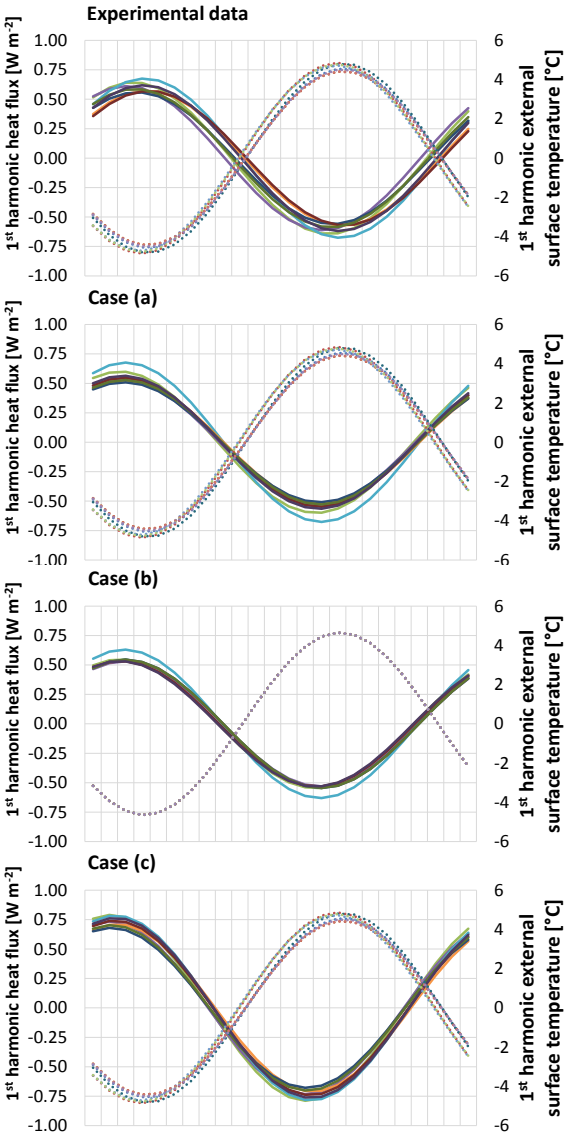

Fig. 5 – First harmonics from day III to X of the heat flux (solid lines, left axis) and of the external surface temperature (dotted lines, right axis) for experimental data, cases (a), (b) and (c).

Calculating the dynamic parameters for cases (a) and (b), we got very close values, with slightly larger standard deviations for case (a) (Tab. 2). For both configurations, Y_{ie} and Δt_{ie} decrease of about 10 % and 3 %, respectively, compared to the calibrated model. Also cases (c) and (d) are close to each other but both are also very close to the EN ISO 13786:2007 analytical solution: indeed, for Y_{ie} the deviation is, respectively, +4 % and +2 % while for Δt_{ie} it is around -1.5 %. Comparing cases (c) and (d) to (a) and (b), the presence of non-stable internal conditions is confirmed to affect the calculated dynamic parameters dramatically, much more than applying non-sinusoidal forcing temperatures to the external

side. Furthermore, the good agreement between the case (d) and EN ISO 13786:2007 analytical solution underlines the numerical model robustness and its adequacy for further in-depth analyses with different forcing signals.

Table 2 – Dynamic parameters for numerical cases (a), (b), (c) and (d).

Case	Y_e [W m^{-2} K^{-1}]	$\Delta(Y_{ie})$ [W m^{-2} K^{-1}]	Δt_{ie} [h]	$\Delta(\Delta t_{ie})$ [h]
(a)	0.121	0.011	10.67	0.23
(b)	0.118	0.007	10.66	0.14
(c)	0.159	0.001	10.05	0.14
(d)	0.156	0.000	10.03	0.02

3.3 Assessment of different forcing temperatures

As showed in Fig. 6, sinusoidal, square and triangle external surface temperatures originate very similar heat fluxes. In particular, for the cases of group (d) all heat fluxes are almost sinusoidal with small differences in phase and amplitude. The wall filters the transmission of almost all harmonics with frequencies higher than that of the first one and this makes small differences between the heat fluxes by different forcing signals built starting from the same first harmonic.

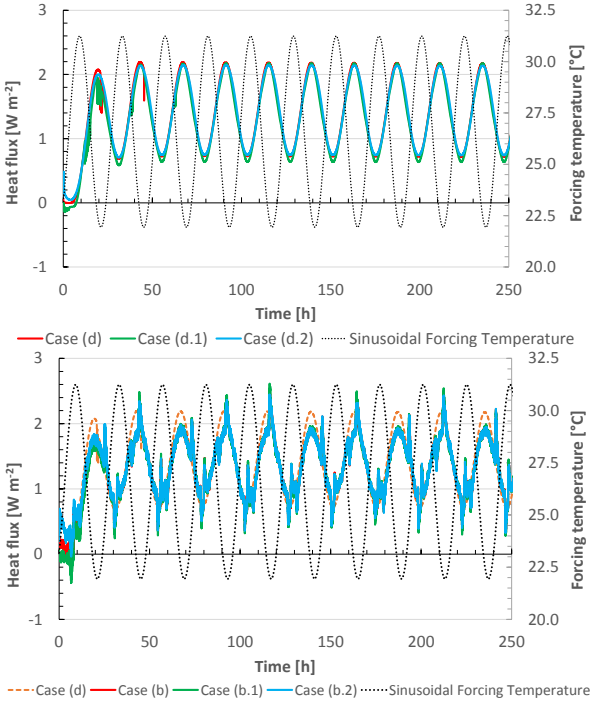

Fig. 6 – Heat fluxes for cases (b), (b.1), (b.2), (d), (d.1) and (d.2).

Comparing group (b) to (d), it can be observed that the internal conditions significantly altered the shape of the heat flux: in particular, neglecting the perturbation due to the air-conditioning units, the amplitude results lower. Mapping amplitude and phase of the first harmonic of the heat flux from days III to X (Fig. 7), we can see different behaviors. Concerning the experimental data and calibrated model, we have variability of around 0.1 W m^{-2} and 0.15 W m^{-2} for the amplitude and 0.35 rad and 0.25 rad for the phase. In cases (b), a periodic forcing signal is adopted and the variability is lowered to 0.1 rad for the phase and small changes are detected for the amplitude. In cases (d), every day the first harmonic of the flux has almost the same amplitude and phase: residual errors are indeed due to numerical model and *FFT* errors. The three different forcing solicitations realized fluxes with differences very small if compared to previous cases. For example, the triangle wave temperature induced a heat flux whose first harmonic has slightly lower phase and amplitude with respect to the other cases.

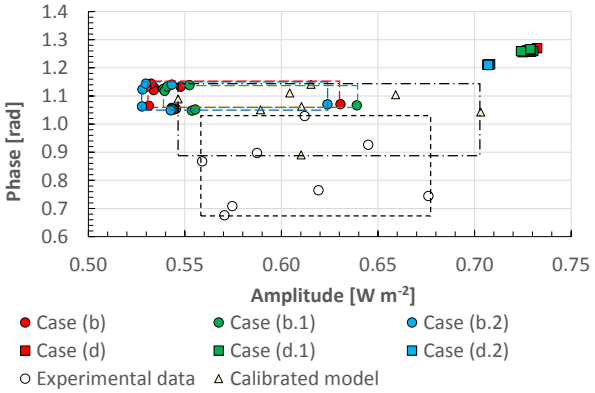

Fig. 7 – Phase and amplitude of the heat fluxes for cases (b), (b.1), (b.2), (d), (d.1) and (d.2) for days from III to X.

Table 3 – Dynamic parameters for numerical cases (b.1), (b.2), (d.1) and (d.2).

Case	Y_e [W m^{-2} K^{-1}]	$\Delta(Y_{ie})$ [W m^{-2} K^{-1}]	Δt_{ie} [h]	$\Delta(\Delta t_{ie})$ [h]
(b.1)	0.120	0.007	10.67	0.14
(b.2)	0.117	0.006	10.66	0.15
(d.1)	0.157	0.000	10.02	0.01
(d.2)	0.152	0.000	10.22	0.00

Considering EN ISO 13786:2007 dynamic parameters, changing the forcing signal has not

remarkable effects: indeed, cases (b.1) and (b.2) have periodic thermal transmittances and time shifts within ±2 % with respect to case (b) results and cases (d.1) and (d.2) have dynamic parameters within ±3 % with respect to case (d) ones.

4. Conclusion

In this work, we exploited a numerical ANSYS Fluent® model to simulate the dynamic behavior of a single layer timber wall during a dynamic test with the modified hotbox apparatus at the Free University of Bozen-Bolzano for the experimental evaluation of EN ISO 13786:2007 dynamic parameters. Once the numerical model was calibrated with experimental results, we focused on the boundary conditions applied to the specimen, considering both actual and constant internal air temperatures and different external surface forcing solicitations. We found that different forcing temperature profiles have little and acceptable effects on the estimation of the dynamic parameter according to the proposed experimental procedure (i.e., we can use non-sinusoidal periodic forcing signals). On the contrary, large sensitivity was registered to the internal conditions, which can affect the final output more than expected. These findings will be used as drivers for the next upgrade of the modified hotbox apparatus in order to improve the accuracy of the experimental results. Further steps of this work will focus on the heat flow meter *HFM* in order to characterize not only the noises that *HFM* introduces but also its response in transient conditions.

5. Acknowledgement

The research leading to these results has received funding from the European Union (FESR 2007-2013) in the framework of the programme "Competitivitá regionale ed occupazionale" of the Autonomous Province of South Tyrol.

References

Asdrubali, F., Baldinelli, G., 2011, Thermal Transmittance measurements with the hot box method: Calibration, experimental procedures, and uncertainty analyses of three different approaches. *Energy & Buildings*, 43: 1618-1626

CEN, 1998, EN 1934:1998 - Thermal performance of buildings - Determination of thermal resistance by hot box method using heat flow meter

CEN, 2007, EN ISO 13786:2007 - Thermal performance of building components - Dynamic thermal characteristics - Calculation methods.

Ferrari, S., Zanotto, V., 2013, The thermal performance of walls under actual service conditions: Evaluating the results of climatic chamber tests. *Construction and Building Materials*, 43: 309-316

Martìn, K., Flores, I., Escudero, C., Apaolaza, A., Sala, J.M., 2010, Methodology for the calculation of response factors through experimental tests and validation with simulation. *Energy & Buildings*, 42: 461–467

Prada, A., Gigli, D.S., Gasparella, A., Baratieri, M., 2013, Energy simulation and design of a hot box suitable for dynamic tests of building envelope components. *Proc. Of BSA 2013 - 1st IBPSA-Italy conference*, Bolzano, Italy, 2013

Press, W.H., Teukolsky, S.A., Vetterling, W.T., Flannery, B.P., 2007, Numerical Recipes 3rd Edition: The Art of Scientific Computing, Cambridge University Press, Cambridge (U.K.)

Sala, J.M., Urresti, A., Martìn, K, Flores, I., Apaolaza, A., 2008, Static and dynamic thermal characterisation of a hollow brick wall: Tests and numerical analysis. *Energy & Buildings*, 40

Sun, C., Shu, D., Ding, G., Zhang, X., Hun, X., 2013, Investigation of time lags and decrement factors for different building outside temperatures. *Energy & Buildings*, 61: 1-7

Ulgen, K., 2002, Experimental and theoretical investigation of effects of wall's thermophysical properties on time lag and decrement factor. *Energy & Buildings*, 34: 273-278

Yesilata, B., Turgut, P., 2007, A simple dynamic measurement technique for comparing thermal insulation performances of anisotropic building materials. *Energy & Buildings*, 39: 1027–1034